International Journal of Engineering Research & Technology (IJERT)
ISSN: 2278-0181
Vol. 5 Issue 07, July-2016

Analysis and Synthesis of Bistable Compliant Mechanisms using Precompressed Beams

Dews Joy, Hong Zhou
Department of Mechanical Engineering
Texas A&M University-Kingsville
Kingsville, Texas, USA

***Abstract*—Bistable mechanisms have two stable equilibrium positions. Power input is not needed for bistable mechanisms to maintain any of their two stable positions. Actuation is only necessary to switch from one stable position to another. Because of their unique features, there are various applications that include switches, valves, closures and many other consumer products. Compliant mechanisms take advantage of elastic deformation to realize mechanism functions. Their jointless structures bring them remarkable merits. Bistable compliant mechanisms achieve bistable behavior based on recoverable deflections of flexible elements instead of relative motions of kinematic joints in conventional rigid-body bistable mechanisms. Precompressed beams with two clamped ends have two symmetric first mode buckled shapes and can be actuated to snap from one buckled shape to another. The two buckled shapes match the two stable equilibrium positions of bistable compliant mechanisms. Because of buckling instability, large deflection and integrated force and motion characteristics, designing precompressed beams for bistable mechanisms is not trivial. In this paper, the first mode buckled shape is derived for a precompressed beam. The critical force is analyzed for a precompressed beam to snap between its two buckled shapes. Precompressed beams are synthesized through thickness modulation to improve their stability. The results from this paper provide a guideline for analyzing and synthesizing precompressed beams as bistable compliant mechanisms.**

Keywords*— *Bistable Mechanism; Compliant Mechanism; Precompressed Beam; Buckling; Stability; Analysis; Synthesis.

I. INTRODUCTION

Bistable mechanisms have two stable equilibrium positions. The energy level is low at both of the two stable positions. There is an instable equilibrium position that has high energy level between the two stable equilibrium positions. Power input is not needed for bistable mechanisms to maintain any of their two stable positions. Actuation is only necessary to switch from one stable position to another [1-2]. Because of the high energy instable equilibrium position, a bistable mechanism will resist itself away from its stable equilibrium position under a certain amount of external disturbance. When a bistable mechanism is actuated and driven away from one stable position, it snaps to another stable position from the instable equilibrium position. Because of their unique features, there are various bistable mechanism applications that include switches, valves, closures and many other consumer products.

Compliant mechanisms take advantage of elastic deformation to realize mechanism functions. Their jointless structures bring them remarkable merits [3-4]. Because of the elimination of kinematic joints, compliant mechanisms fits well for mechanism miniaturization and micro-electro-mechanical system (MEMS). Compliant mechanisms have been widely used for MEMS applications [5].

Bistable behavior is achieved in bistable compliant mechanisms based on recoverable deflections of flexible elements instead of relative motions of kinematic joints in conventional rigid-body bistable mechanisms. Bistable compliant mechanisms carry advantages from the jointless structures of compliant mechanisms and allow MEMS to be developed with improved energy efficiency and positioning accuracy [6].

Precompressed beams with two clamped ends have two symmetric first mode buckled shapes and can be actuated to snap from one buckled shape to another. The two buckled shapes match the two stable equilibrium positions of bistable compliant mechanisms. Precompressed beams have been modeled, analyzed, fabricated and tested as bistable compliant mechanisms [7-10]. The actuation for a precompressed beam to snap between two stable equilibrium positions can be either a force or moment [11]. The actuator location of a precompressed beam can be at the clamped end or between the two clamped ends [12]. The support for clamped ends can be firm or flexible. When the supporting angle of a clamped beam exceeds a critical angle, the bistability of the beam is lost and only one stable equilibrium position can be reached [13].

When a precompressed double-clamped beam is used as a bistable compliant mechanism, the two stable equilibrium positions correspond to its two buckled shapes that have low energy level. If the initial undeformed beam is straight, the longitudinal compression load applied at the ends of the beam must be no lower than its Euler's critical load [14]. Otherwise, the beam will not buckle and there is no stable equilibrium position. When a beam is buckled, obtaining its post-buckling shape is not trivial. Unlike Euler's critical load, there is no analytical formula that directly leads to the buckled beam shape. For a buckled beam to snap from one stable position to another stable position, the actuation force or moment has to be beyond its critical value or the beam will not snap. Calculating the critical snapping force or moment for a buckled beam is not straightforward. Because of buckling instability, large deflection and integrated force and motion characteristics, synthesizing bistable compliant mechanisms is much more challenging than rigid-body bistable mechanisms. Motivated by these challenges, this paper aims at providing a guideline and systematic approach for analyzing and synthesizing precompressed double-clamped beams that are used as bistable compliant mechanisms.

The remainder of the paper is organized as follows. The beam buckling analysis is presented in section II. The analysis on bistable compliant mechanisms is provided in section III. Section IV is on the synthesis of bistable compliant mechanisms. Conclusions are finally drawn in section V.

II. BEAM BUCKLING ANALYSIS

The initially straight beam shown in Figure 1 has uniform rectangular cross section with in-plane thickness of t and out-of-plane width of b. The original undeformed length of the beam is L_0. Its left end is clamped. The right end of the beam has no rotation and can only translate longitudinaly. The beam is under axial compression with force P applied at its right end. After the right end of the beam is compressed by ΔL, the right end is also clamped. The deformed beam becomes a double-clamped beam and is shown in Figure 2. The length of the deformed beam is L that meets equation $L = L_0 - \Delta L$. Figure 3 shows the free-body diagram of the loads acting on the right portion of the double-clamped beam.

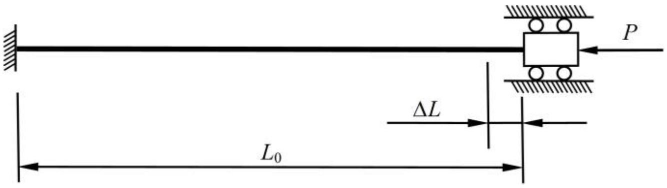

Fig. 1 An initially straight beam.

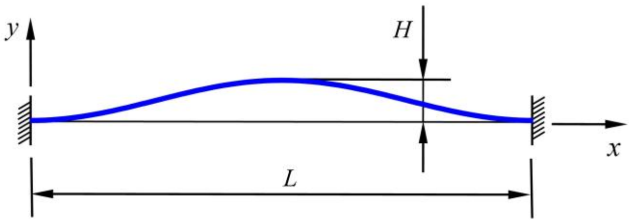

Fig. 2 The double-clamped beam.

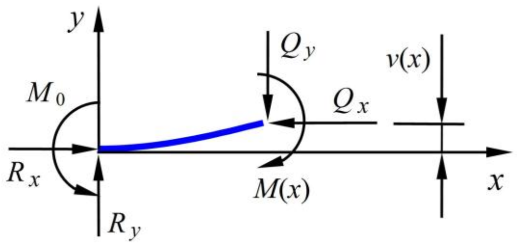

Fig. 3 The free-body diagram of the double-clamped beam.

According to Euler–Bernoulli beam theory [15], the deflection of a beam is related to its bending moment by $M(x) = -EIv''(x)$. E here is Young's modulus of the beam material. I is the area moment of inertia of the cross section of the beam. For rectangular cross section, I is calculated by $I = \frac{bt^3}{12}$. Equilibrium of the beam section results in the following equation [16].

$$M(x) = -EIv''(x) = M_0 + R_x v(x) - R_y x \tag{1}$$

R_x in equation (1) equals the applied axial compressive force P in Figure 1. Rearranging equation (1) yields the following equation.

$$\frac{d^2 v(x)}{dx^2} + \frac{P}{EI} v(x) = \frac{R_y}{EI} x - \frac{M_0}{EI} \tag{2}$$

There are four boundary conditions from the double-clamped beam in Figure 2 that can be used to solve equation (2). These boundary conditions are expressed in the following two equations.

$$v(0) = v(L) = 0 \tag{3}$$

$$\left(\frac{dv(x)}{dx}\right)_{x=0} = \left(\frac{dv(x)}{dx}\right)_{x=L} = 0 \tag{4}$$

In order for equation (2) to have nonzero solutions, the following equation has to be satisfied [15-16].

$$\sin\left(\frac{kL}{2}\right)\left[\sin\left(\frac{kL}{2}\right) - \frac{kL}{2}\cos\left(\frac{kL}{2}\right)\right] = 0 \tag{5}$$

k in equation (5) is defined by $k = \sqrt{P/EI}$. Equation (5) leads to two groups of nonzero solutions. The first group is from $\sin\left(\frac{kL}{2}\right) = 0$. This condition leads to k value as $k_i L = (1+i)\pi, i = 1, 3, 5, \cdots$. The solutions of this group can be expressed as:

$$v_i(x) = A_i\left(1 - \cos(k_i x)\right) \tag{6}$$

The second group of solutions is from condition $\sin\left(\frac{kL}{2}\right) - \frac{kL}{2}\cos\left(\frac{kL}{2}\right) = 0$, which means $\tan\left(\frac{kL}{2}\right) = \frac{kL}{2}$. This leads to $k_j L = 2.86\pi, 4.92\pi, 6.94\pi, \cdots, j = 2, 4, 6, \cdots$. The solutions of the second group are expressed as follows.

$$v_j(x) = B_j\left(1 - \frac{2x}{L} - \cos(k_j x) + \frac{2}{k_j L}\sin(k_j x)\right) \tag{7}$$

A_i and B_j in equations (6) and (7) are arbitrary constants to be determined on the amplitudes of the deflection functions.

When i in Equation (6) is 1, we have $k_1 L = (1+1)\pi = 2\pi$. Substituting $k = \sqrt{P/EI}$ into the equation yields the following equation.

$$P = \frac{4\pi^2 EI}{L^2} \tag{8}$$

The P value calculated from Equation (8) is the Euler's critical load on the double-clamped beam, which is commonly represented as P_{cr}. When $P > P_{cr}$, the initially straight beam will be buckled. The first mode buckled shape is $v_1(x)$. From Equation (6), $v_1(x)$ is represented as follows.

$$v_1(x) = A_1\left(1 - \cos\left(2\pi\frac{x}{L}\right)\right) \tag{9}$$

International Journal of Engineering Research & Technology (IJERT)
ISSN: 2278-0181
Vol. 5 Issue 07, July-2016

When A_1 in Equation (9) changes its sign from positive to negative or vice versa, the buckled shape of $v_1(x)$ is flipped with respect to x axis. So there are two symmetric first mode buckled shapes that are shown in Figure 4.

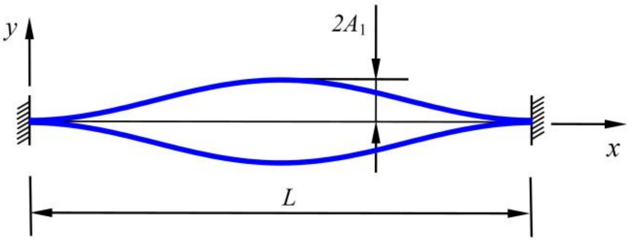

Fig. 4 The two symmetric first mode buckled shapes.

When j in Equation (7) is 2, we have the second mode buckled shape $v_2(x)$. From Equation (7), $v_2(x)$ can be represented as follows.

$$v_2(x) = B_2\left(1-\frac{2x}{L}-\cos\left(2.86\pi\frac{x}{L}\right)+\frac{2}{2.86\pi}\sin\left(2.86\pi\frac{x}{L}\right)\right) \quad (10)$$

Figure 5 shows the two symmetric second mode buckled shapes.

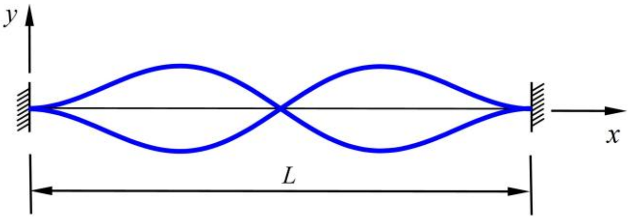

Fig. 5 The two symmetric second mode buckled shapes.

The third or any other higher mode buckled shape can be derived from either Equation (6) or (7). Like any other buckled mechanical system, a double-clamped buckled beam tends to move towards the lowest energy configuration. The first mode buckled shape is stable and has the lowest energy level among all buckled shapes. Without input power, a buckled double-clamped beam stays at one of its two symmetric first mode buckled shapes.

For an initially straight slender beam, its post-buckling shape is shown in Figure 2. If the lateral deflection amplitude is H, the deflection equation is then:

$$y(x) = \frac{H}{2}\left(1-\cos\left(2\pi\frac{x}{L}\right)\right) \quad (11)$$

The lateral deflection comes from the longitudinal deformation ΔL as shown in Figure 1. If the buckled slender beam is considered as incompressible and inextensible, the arc length of the buckled beam equals its original straight length of L_0. The following equation can then be established.

$$\int_0^L \sqrt{1+\left(y'(x)\right)^2}\,dx = L_0 \quad (12)$$

In the above equation, $L = L_0 - \Delta L$ and $y'(x) = \frac{H}{L}\pi\sin\left(2\pi\frac{x}{L}\right)$.

With given L_0 and L, H can be solved from Equation (12) by using numerical integration method such as Gauss Quadrature [17].

III. BISTABLE COMPLIANT MECHANISM ANALYSIS

The buckled shape of a double-clamped beam can be directly analyzed by finite element analysis software ANSYS [18-19]. Figure 6 shows the solid model of an initially straight uniform beam with $L_0 = 150$ mm, $t = 1$ mm, and $b = 8$ mm. The material of the beam is engineering plastic with Young's modulus of 2000 MPa, Poisson's ratio of 0.45, and yield strength of 60 MPa.

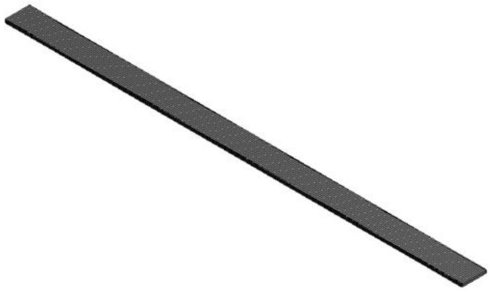

Fig. 6 The solid model of an initially straight beam.

The above beam model is created by using ANSYS Design Modeler [20] that provides modeling tools for geometry creation and modification, and is an application of ANSYS Workbench [21].

After the beam is modeled in ANSYS Design Modeler, it is analyzed within ANSYS Mechanical [22], another application of ANSYS Workbench. The left end of the beam is fixed. Its right end is compressed by 5 mm with all rotations constrained. Figure 7 shows the deformed beam that has its first mode buckled shape. As shown in Figure 7, the maximum vertical deflection of the beam is 17.148 mm that occurs at the middle of the beam. The Euler's buckling load calculated from Equation (8) is 2.3395 N. The horizontal reaction force at the two ends in Figure 7 is 2.3227 N, which is very close to the calculated Euler's buckling load.

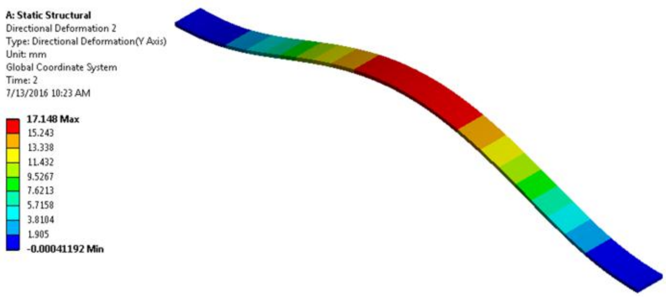

Fig. 7 The first mode buckled shape of the beam.

At the maximum deflection place of the buckled beam, a step by step downward input displacement of 1 mm is applied. At each input displacement step, the input force (the reaction force at the input displacement place in ANSYS), the deformed beam shape and the stress distribution are obtained from ANSYS Mechanical. When the downward input displacement is less than or equal to 17 mm, the required input force is also downward. However, the required input force changes its direction and becomes upward when the input downward displacement is 18 mm or above. The reversed

International Journal of Engineering Research & Technology (IJERT)
ISSN: 2278-0181
Vol. 5 Issue 07, July-2016

input force means that the deformed beam will snap by itself. In order to stop the beam snapping, an upward input force has to be applied. When the input force is zero, the deformed shape of the beam has its second mode buckled shape that is an instable equilibrium position, which is shown in Figure 8.

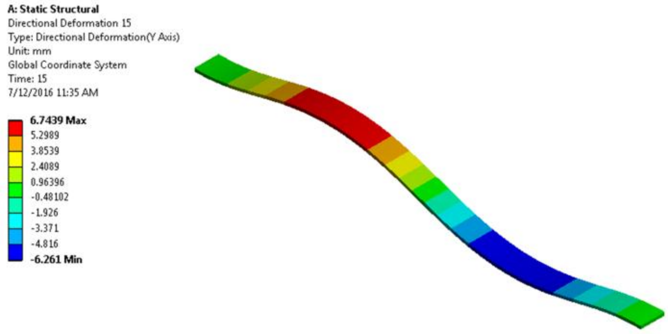

Fig. 8 The second mode buckled shape of the beam.

With the input displacement increasing, the beam continues its downward deflection. The maximum downward input displacement is set to make the mid-point of the beam have downward displacement of -17.148 mm, which is symmetric to the upward displacement of 17.148 mm. With the maximum downward input displacement, the deformed beam has its downward first mode buckled shape, which is shown in Figure 9.

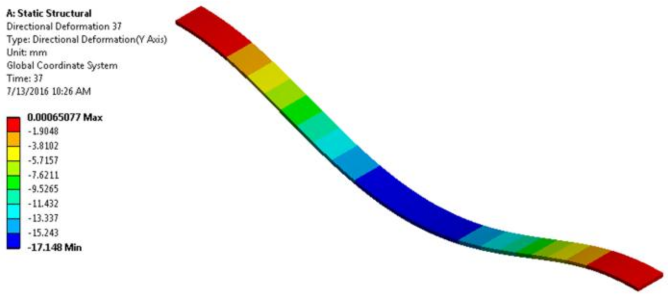

Fig. 9 The downward first mode buckled shape of the beam.

At each input displacement step, the required input force is analyzed. The maximum downward input force is 1.56 N. It occurs when the input displacement is 1 mm, which is near the first mode buckled shape. Figure 10 shows the beam shape that needs the maximum input force to have the deformed shape.

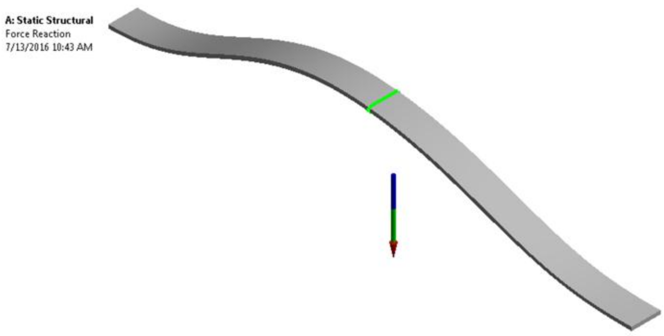

Fig. 10 The beam shape for the maximum input force.

The maximum input force is usually called the critical force for the buckled beam to snap from its upward first mode buckled shape to the symmetric downward first mode buckled shape. If the input force or external disturbance force is less than the critical force, the buckled beam will not snap. It will recover to its original buckled shape when the disturbance force is released. The stability of the bistable compliant mechanism from the double-clamped buckled beam closely relates to the critical force. The higher is the critical force, the better is the stability.

At each input displacement step, the von Mises stress (the equivalent stress in ANSYS) is analyzed. The maximum stress within the beam is required to be below the allowable stress value of the beam. The maximum stress of the buckled beam is 23.863 MPa, which is shown in Figure 11 together with its deformed beam shape.

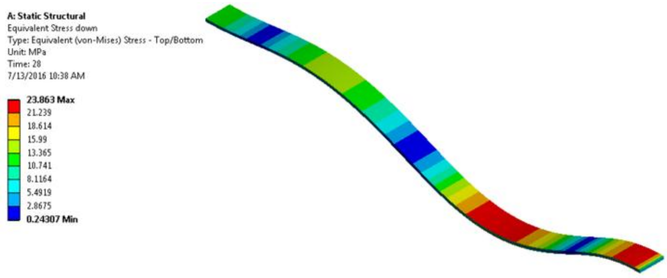

Fig. 11 The maximum stress and the deformed beam.

The buckled shapes, critical force, and maximum stress of other double-clamped beams can be similarly analyzed.

IV. BISTABLE COMPLIANT MECHANISM SYNTHESIS

Synthesis of a bistable compliant mechanism is to select mechanism dimensions and decide two stable equilibrium positions to meet the needs and requirements for a specific application. For a double-clamped buckled beam used as a bistable compliant mechanism, its dimensions include cross sectional sizes (t and b) and initially straight beam length (L_0). Any change of the three dimensions will more or less affect the mechanism.

In Section III, the thickness t of the analyzed double-clamped beam is 1 mm. If t is increased to 1.35 mm and other aspects are kept as the same, the Euler's buckling load from Equation (8) is now 5.7560 N that is more than doubled compared with that (2.3395 N) of the beam in Section III. The first mode buckled shape is shown in Figure 12.

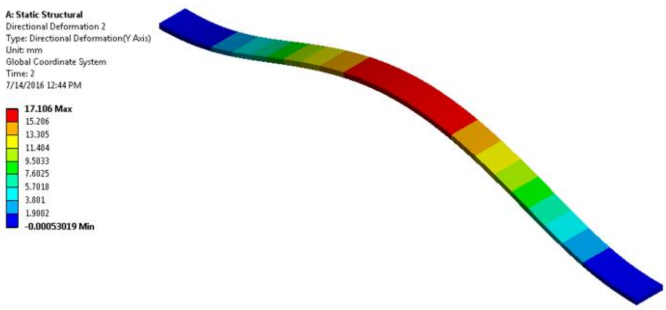

Fig. 12 The first mode buckled shape of the beam with an increased thickness.

The maximum vertical deflection of the beam in Figure 12 is 17.106 mm, which is almost the same as that (17.148 mm) of the beam with thickness of 1 mm. The critical force is 8.85 N, which is much higher than that (1.56 N) of the beam with thickness of 1 mm. The maximum stress is 42.191 MPa, which is way above that (23.863 MPa) of the beam with thickness of 1 mm.

International Journal of Engineering Research & Technology (IJERT)
ISSN: 2278-0181
Vol. 5 Issue 07, July-2016

When the beam thickness is increased, the Euler's buckling load, the critical force and the maximum stress of the double-clamped buckled beam will increase sharply.

When the beam thickness t is decreased from 1 mm to 0.65 mm. The Euler's buckling load from Equation (8) is now 0.6425 N that is much lower than that (2.3395 N) of the beam in Section III. The first mode buckled shape shown is shown in Figure 13.

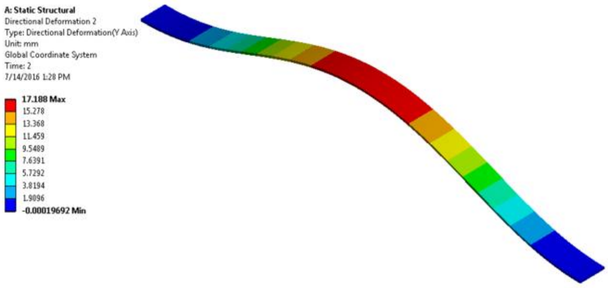

Fig. 13 The first mode buckled shape of the beam with an decreased thickness.

The maximum vertical deflection of the beam in Figure 13 is 17.188 mm, which is almost the same as that (17.148 mm) of the beam with thickness of 1 mm. The critical force is 0.51 N, which is much lower than that (1.56 N) of the beam with thickness of 1 mm. The maximum stress is 16.07 MPa, which is smaller than that (23.863 MPa) of the beam with thickness of 1 mm.

When the beam thickness is decreased, the Euler's buckling load and critical force of the double-clamped buckled beam will decrease sharply. The maximum stress of the beam will decrease, but not sharply.

With the same dimensions, the performance of a double-clamped buckled beam will also be changed when its compression ΔL is increased or decreased. In Section III, compression ΔL of the analyzed double-clamped beam is 5 mm. If ΔL is increased to 6 mm and other aspects are kept as the same, the first mode buckled shape is shown in Figure 14.

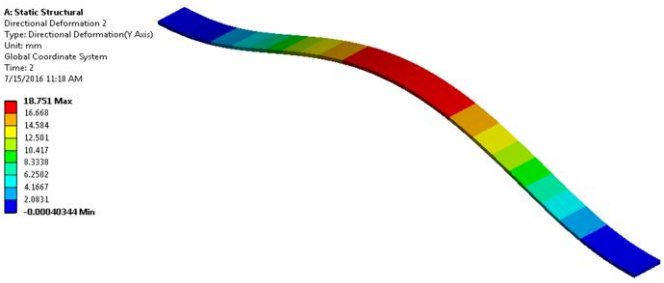

Fig. 14 The first mode buckled shape of the beam with an increased compression.

The maximum vertical deflection of the beam in Figure 14 is 18.751 mm that is higher than that (17.148 mm) of the beam with compression of 5 mm. The critical force is 1.73 N that is also higher than that (1.56 N) of the beam with compression of 5 mm. The maximum stress is 26.096 MPa, which is above that (23.863 MPa) of the beam with compression of 5 mm.

When the beam compression is increased, the Euler's buckling load is the same since the beam dimensions are not changed, but the deflection, the critical force and the maximum stress of the double-clamped buckled beam will increase.

If ΔL is decreased to 4 mm and other aspects are kept as the same, the first mode buckled shape is shown in Figure 15.

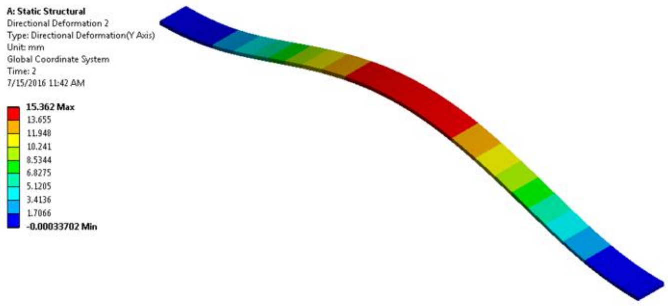

Fig. 15 The first mode buckled shape of the beam with an decreased compression.

The maximum vertical deflection of the beam in Figure 15 is 15.362 mm that is lower than that (17.148 mm) of the beam with compression of 5 mm. The critical force is 1.40 N that is also lower than that (1.56 N) of the beam with compression of 5 mm. The maximum stress is 21.347 MPa, which is below that (23.863 MPa) of the beam with compression of 5 mm.

When the beam compression is decreased, the deflection, the critical force and the maximum stress of the double-clamped buckled beam will decrease.

The double-clamped buckled beams analyzed above all have uniform cross section. It is not necessary for an initially straight beam to have a uniform cross section. A nonuniform beam model is shown in Figure 16 in which the in-plane thickness is nonuniform and controlled by three independent thickness parameters (t_1, t_2 and t_3). The upper and bottom curves are symmetric spline interpolation curves [23] that are defined by five interpolation points and controlled by three thickness parameters. The five interpolation points are evenly distributed along the beam axis. As shown in Figure 16, the left half of the beam is symmetric to its right half. When the three thickness parameters have the same value, the nonuniform beam becomes uniform.

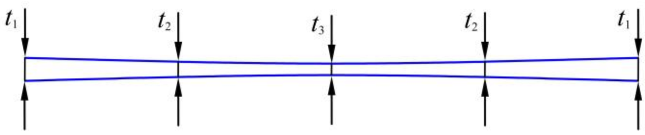

Fig. 16 A general nonuniform beam.

The thickness t of the double-clamped beam analyzed in Section III is uniformly 1 mm. When t_3 is increased to 1.35 mm while t_1 and t_2 are kept as 1 mm, the first mode buckled shape of the nonuniform beam is shown in Figure 17. The beam compression is the same as 5 mm.

The maximum vertical deflection of the nonuniform beam in Figure 17 is 16.654 mm that is lower than that (17.148 mm) of the uniform beam with thickness of 1 mm. The Euler's buckling load from ANSYS that is the horizontal reaction force at the two ends in Figure 17 is 3.1094 N, which is higher than that (2.3227 N) of the uniform beam. The critical force is 2.37 N that is also higher than that (1.56 N) of the uniform beam. The maximum stress is 29.647 MPa, which is above that (23.863 MPa) of the uniform beam.

International Journal of Engineering Research & Technology (IJERT)
ISSN: 2278-0181
Vol. 5 Issue 07, July-2016

When the beam thickness is locally increased near its middle part, the Euler's buckling load, the critical force and the maximum stress of the double-clamped buckled beam will increase while the beam deflection will decrease. With the general nonuniform beam model shown in Figure 16, other nonuniform cases can be similarly analyzed.

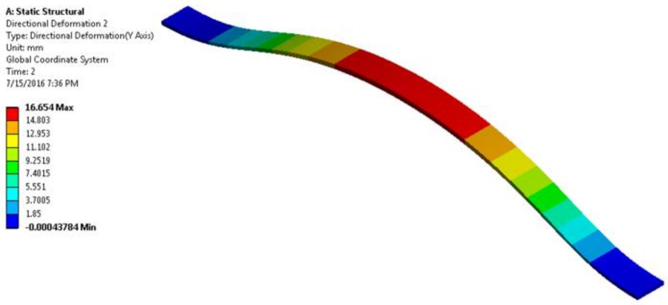

Fig. 17 The first mode buckled shape of the beam with nonuniform cross section.

V. CONCLUSIONS

When a double-clamped buckled beam is used as a bistable compliant mechanism, its Euler's critical load, maximum lateral deflection, first mode buckled shape, critical force play crucial roles for its bistability. The maximum stress within the buckled beam and during its snapping process is important for the beam to avoid failure. This paper provides an effective approach to analyze double-clamped buckled beams and obtain their buckled shapes and other critical or maximum values.

The beam thickness and compression of a double-clamped buckled beam significantly affects its bistability. Both increase and decrease of beam thickness and compression are analyzed in the paper to observe their effects on Euler's critical load, maximum lateral deflection, first mode buckled shape, critical force and maximum stress. A general nonuniform beam model is introduced in the paper to synthesize double-clamped buckled beams as bistable compliant mechanisms.

ACKNOWLEDGMENT

The authors of this paper gratefully acknowledge the research instrument support of the US National Science Foundation under Grant No. 1337620. Any opinions, findings, recommendations or conclusions expressed in this paper are those of the authors and do not necessarily reflect the views of the US National Science Foundation.

REFERENCES

[1] P.G. Opdahl, B.D. Jensen, L.L. Howell, “An Investigation into Compliant Bistable Mechanisms,” Proceedings of the ASME 1998 International Design Engineering Technical Conferences, Atlanta, USA, DETC98/MECH-5914, 1998.

[2] B.D. Jensen, L.L. Howell, “Identification of Compliant Pseudo-Rigid-Body Mechanism Configurations Resulting in Bistable Behavior,” Proceedings of the ASME 2000 International Design Engineering Technical Conferences & Computers and Information in Engineering Conference, Baltimore, USA, DETC2000/MECH-14147, 2000.

[3] L.L., Howell, Compliant Mechanisms. Hoboken, NJ: Wiley, 2001.

[4] L.L., Howell, S.P., Magleby, B.M., Olsen, Handbook of Compliant Mechanisms. Hoboken, NJ: Wiley, 2013.

[5] G.K., Ananthasuresh, Optimal Synthesis Methods for MEMS. norwell, Massachusetts 02061 USA: Kluwer Academic Publishers, 2003.

[6] B.D. Jensen, L.L. Howell, L.G. Salmon, "Design of Two-Link, In-Plane, Bistable Compliant Micro-Mechanisms," ASME Journal of Mechanical Design, 1999, 121(3): 416-423.

[7] M. Vangbo, Y. Backlund, "A Lateral Symmetrically Bistable Buckled Beam," Journal of Micromechanics and Microengineering, 1998, 8(1): 29-32.

[8] M. Vangbo, "An Analytical Analysis of a Compressed Bistable Buckled Beam," Sensors and Actuators, 1998, 69(3): 212-216.

[9] P. Cazottes, A. Fernandes, J. Pouget, M. Hafez, "Bistable Buckled Beam: Modeling of Actuating Force and Experimental Validations," ASME Journal of Mechanical Design, 2009, 131(10): 101001.

[10] J. Zhao, J. Jia, X. He, H. Wang, "Post-Buckling and Snap-Through Behavior of Inclined Slender Beams," ASME Journal of Applied Mechanics, 2008, 75(4): 041020.

[11] R.H. Plaut, L.N. Virgin, "Vibration and Snap-Through of Bent Elastica Strips Subjected to End Rotations," ASME Journal of Applied Mechanics, 2009, 76(4): 041011.

[12] J. Cleary, H. Su, "Modeling and Experimental Validation of Actuating a Bistable Buckled Beam Via Moment Input," ASME Journal of Applied Mechanics, 2015, 82(5): 051005.

[13] J. Beharic, T.M. Lucas, C.K. Harnett, "Analysis of a Compressed Bistable Buckled Beam on a Flexible Support," ASME Journal of Applied Mechanics, 2014, 81(8): 081011.

[14] S.R., Schmid, B.J., Hamrock, B.O., Jacobson, Fundamentals of Machine Elements, Third Edition. 6000 Broken Sound Parkway, Boca Raton, FL: CRC Press, 2014.

[15] S.P. Timoshenko, J.M. Gere, Theory of Elastic Stability. Mineola, New York: Dover Publications, 2009.

[16] I. Doghri, Mechanics of Deformable Solids. 233 Spring Street, New York: Springer, 2000.

[17] W.Y. Yang, W. Cao, T.S. Chung, J. Morris, Applied Numerical Methods Using MATLAB. Hoboken, NJ: Wiley, 2005.

[18] E.H., Dill, The Finite Element Method for Mechanics of Solids with ANSYS Applications. 6000 Broken Sound Parkway, NY: CRC Press, 2012.

[19] S., Moaveni, Finite Element Analysis Theory and Application with ANSYS, Fourth Edition, Upper Saddle River, NJ: Pearson, 2015,

[20] ANSYS, Design Modeler User's Guide, Canonsburg, PA: ANSYS, 2015.

[21] H.H., Lee, Finite Element Simulations with ANSYS Workbench 16, 5442 Martway Drive, Mission, KS: SDC Publications, 2015.

[22] ANSYS, ANSYS Mechanical User's Guide, Canonsburg, PA: ANSYS, 2015.

[23] D. Salomon, Curves and Surfaces for Computer Graphics. 233 Spring Street, New York: Springer, 2006.